

Solid Phase-Enhanced Photothermal Lensing with Mesoporous Polymethacrylate Matrices for Optical-Sensing Chemical Analysis

Dmitry A. Nedosekin,^a Nadezhda V. Saranchina,^b Aleksey V. Sukhanov,^b Nataliya A. Gavrilenko,^b Ivan V. Mikheev,^c Mikhail A. Proskurnin^{c,*}

^a Department of Otolaryngology, University of Arkansas for Medical Sciences, Little Rock, AR 72205, USA

^b Tomsk Polytechnical University, Russia, 634050, Lenin Avenue 30, Tomsk, Russia

^c Chemistry Department, M.V. Lomonosov Moscow State University, Leninskie Gory, 119991, GSP-1 Moscow, Russia

Procedures for the photothermal lens determination of metals and organic compounds, on the basis of solid-phase mesoporous optical-sensing materials (polymethacrylate [PMA]) matrices with immobilized reagents, were developed. These procedures combine (i) selective and efficient preconcentration of trace substances to be analyzed in specially designed and synthesized transparent mesoporous PMA plates; (ii) sensitive determination with the reliable and traceable photometric reactions previously developed for classical spectrophotometry; and (iii) the sensitivity enhancement of photothermal lens detection in polymers, which provides at least a ten-fold increase in sensitivity compared with solutions due to polymer thermo-optical properties (solid phase-enhanced thermal lensing). It is shown that the overall sensitivity of photothermal lens measurements in PMA matrices is two orders higher than photometric absorbance measurements for the same excitation source power, which is in good agreement with the expected theoretical sensitivities. Changes in the preparation of transparent PMA plates and analytical procedures for photothermal measurements compared with spectrophotometry are discussed. PMA matrices modified with various analytical reagents were applied to trace determination of mercury(II), Fe(II), Ag(I), Cu(II), and ascorbic acid, with subnanomolar to nanomolar limits of detection.

Index Headings: Photothermal spectroscopy; Thermal lens spectrometry; Solid-phase spectrophotometry; Optical-sensing materials; Trace determination; Sensitivity comparison.

INTRODUCTION

Solid-phase spectrophotometry (SPS) is rapidly developing as a major method of analytical chemistry.¹ It uses the same laws and instruments as conventional spectrophotometry and can be used for various samples, from transparent solids^{2–5} to films⁶ and resins.⁷ However, the materials used in SPS are rather limited, and this seriously narrows the applicability of the method in chemical analysis, as only few reactions can be used. A strategy to seriously enhance the applicability of SPS is the use of solid-phase sensible materials.^{2,8} These materials are based on the preparation of specially designed mesoporous (bulk absorbing) or surface-enhanced polymer or glass matrices,^{2,3,8–13} with grafted-absorbed photometric reagents. Moreover, these materials not only have a significant merit in conventional spectrophotometry, but are also very advantageous for the combination with photothermal (PT), especially photothermal lens, spectrometry (thermal lens spectrometry

[TLS]).¹⁴ In TLS, ten-fold enhancement in sensitivity in solid-phase analytical matrices, especially polymers compared with aqueous solutions, is achieved due to advantageous thermo-optical properties of these materials (solid-phase-enhanced thermal lens spectrometry [SPETLS]),^{15–18} and promising applications of polymer-based reactions were shown previously.^{14,19} Furthermore, the preparation of presynthesized solid-phase sensible materials usually provides low reagent blanks (especially compared with reactions in solutions), which has a drastic enhancement in photothermal limits of detection.²⁰

In this paper, we summarize the SPETLS applications of several photometric reactions with mesoporous polymethacrylate (PMA) matrices previously optimized for SPS.^{12,17,18,20–22} They (i) combine the immobilization of well known analytical reagents in a solid phase, without degrading matrix transparency and reagent reactivity; (ii) provide good preconcentration factors;^{7,8,15,23–25} and (iii) show good sensitivity of analytical determination of various entities, even at standard analytical instrumentation.^{2,7,15,16,21,22,25–28} They provide a significant advantage over commercially available polymers, both as chemical sorbents and from the point of photothermal sensitivity due to their thermo-optical parameters.^{26,29} In our previous paper,²⁴ we showed the analytical possibilities of PMA in SPETLS for two model cases. The aim of this paper is to extend these findings to various-type procedures and to estimate the general advances of the technique.

MATERIALS AND METHODS

Reagents and Solvents. All used reagents and solvents were at least of analytical grade. We used doubly distilled deionized water (specific resistance, not less than 18.2 MΩ cm) and carbon tetrachloride, chemically pure grade. The following reactants and solvents were used throughout: ammonium Fe(II) sulfate, Cu(II) sulfate, mercury(II) sulfate, Ag(I) nitrate, sodium chloride, potassium hexacyanoferrate(II), and potassium hexacyanoferrate(III), all analytical grade; sulfuric acid, chemically pure grade; nitric acid, chemically pure grade; phosphoric acid, chemically pure grade; sodium hydroxide, chemically pure grade; Fe(II) *tris*(1,10-phenanthroline) sulfate (Chemical Abstracts Service [CAS] no. 14 634-91-4), analytical grade; 1,10-phenanthroline monohydrate (CAS no. 5144-89-8), chemically pure grade; dithizone (CAS no. 60-10-6), analytical grade, and sodium salt of 2,6-dichlorophenolindophenol (CAS no. 620-45-1), analytical grade. All salts of chemically pure and analytical grade were used throughout without additional purification.

Stock 2 M solution of m(II) was prepared by dissolving a

Received 2 August 2012; accepted 19 February 2013

* Author to whom correspondence should be sent. E-mail: proskurnin@gmail.com.

DOI: 10.1366/12-06812

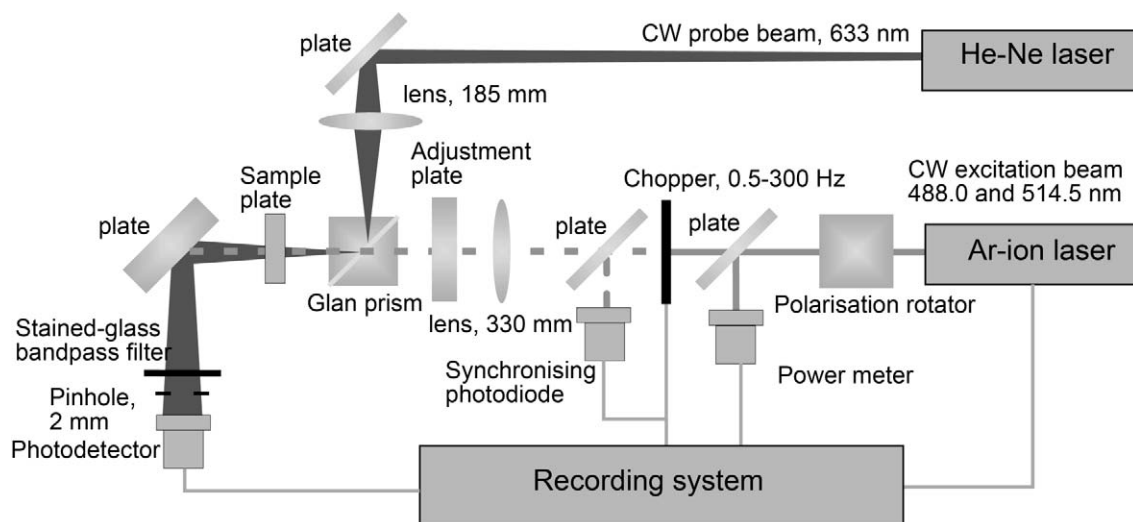


Fig. 1. Block diagram of thermal lens signal generation in the coaxial, dual-beam, far-field thermal lens spectrometer.

weighed portion of metal mercury in diluted nitric acid. Stock solutions of other metals (1 mg/mL) were prepared by dissolving weighed portions of salts in 0.01 M acids.^{21,26} The 2×10^{-3} M working solution of dithizone was prepared by dissolving a weighed portion of the reagent in 1 M NaOH. Borate buffer solutions were prepared from 25 mM sodium borate with 1% (wt/vol) NaN_3 , pH 7.8. Acetate buffer solutions were prepared from 10 mM sodium acetate with 10 mM hydrochloric acid, pH 4.7. All the working solutions were prepared daily before the experiments in doubly distilled water. All the glassware and photometric cells were washed with concentrated chemically pure nitric acid and thoroughly washed with doubly distilled water.

Reagents were immobilized into PMA platelets by adsorption from a solution in the batch mode. In the case of Pb(II) diethyldithiocarbamate and Cu(II) dithizonate, a platelet first soaked in the working solutions of sodium diethyldithiocarbamate and dithizone, respectively. Next, the modified platelet was immersed in aqueous solution of Pb(II) and Cu(II), respectively.

Procedures. Procedure 1. Polymethacrylate Matrix Synthesis. Transparent 10×10 cm PMA plates (thickness, 0.60 ± 0.04 mm) were prepared by radical block polymerization of methacrylate, according to the patent.¹¹ Next, these plates were cut as 6.0×8.0 mm working platelets (weight, ca. 0.05 g) for analyses.

Procedure 2. Matrix Thermal Conditioning. To diminish light scattering, working PMA platelets were placed between two subject microscopic glass plates and heated to 60°C with a UT-08 flat heater, with a slight squeeze of the upper glass plate for 2 min, and then cooled. The procedure was repeated if needed.

Procedure 3. Metal Determination. Unless otherwise stated, the details for the procedures are reported elsewhere.^{2,8,12,26,27,29} A PMA matrix with the immobilized reagent was immersed in a 50–100 mL of the analyte solution (depending on the metal) after adjusting its pH (and after adding a reductant, ascorbic acid, for Fe(III)) and shaken with a laboratory shaker for 5–30 min. Next, the matrix was removed and air dried. Sample absorbances were measured in the maxima of absorption bands of the formed substances in PMA

(490 nm for mercury, 510 nm for Fe, 520 nm for Ag, and 430 nm for Cu); thermal lens signal was measured at 514.5 nm (excitation power, 40–100 mW; chopper frequency, 1 Hz) for Fe(II), Cu(II), and Ag and at 488 nm (excitation power, 100 mW; chopper frequency, 1 Hz) for mercury(II). The concentration of residual Ag in the solution was determined by spectrophotometry.²⁵

Procedure 4. Ascorbic Acid Determination. PMA matrix with immobilized 2,6-dichlorophenolindophenol was immersed in 50 mL of an ascorbic acid solution at pH 3 and shaken with a laboratory shaker for 15 min. Next, the matrix was removed and air-dried. Absorbance of samples was measured at the absorption band maximum of 2,6-dichlorophenolindophenol in PMA (550 nm); thermal lens signal was measured at 514.5 nm (excitation power, 100 mW; frequency, 0.4 Hz).

Thermal Lens Setup. A mode-mismatched dual-laser, parallel-beam thermal lens spectrometer with a single-channel, far-field detection system (Fig. 1) was used.^{30,31} The selection of the instrument parameters (linear dynamic range, optical-scheme design, instrumental sensitivity, etc.) is summarized in Table I and discussed elsewhere.³¹ The principle is based on recording an excitation laser-induced (Innova 90-6, Coherent, Palo Alto, CA) refractive heterogeneity (thermal lens effect), causing defocusing of a collinear He–Ne laser probe beam (SP-106-1, Spectra Physics, Eugene, OR) and hence a reduction in the probe beam intensity at its center, as detected by a far-field photodiode (supplied with a KS-11 stained-glass bandpass filter and a 2 mm-diameter pinhole).³² The thermal lens spectrometer has a linear dynamic range of the signal of four orders of magnitude (the corresponding range of absorption coefficients for 10 mm optical pathways is 1×10^{-6} to 2×10^{-2} cm^{-1}) and the response time of 0.05–2 s. The application of the spectrometer for solid samples was described previously.³⁰

Auxiliary Measurements. Absorption spectra and absorbance of PMA matrix were registered on a Specol 21 and a Shimadzu UV mini-1240 spectrophotometers against a polymer plate prepared under the same conditions, without reagents. The pH values were measured by an inoLab pH level 1 pH meter (Weilheim, Germany) with a glass pH-selective electrode (precision $\pm 5\%$). The beam-intensity profiles and waist sizes for both beams were estimated with an M2-200 Advanced PC

TABLE I. Experimental parameters for the optical-scheme configuration of the dual-beam spectrometer, $T = 293$ K.

Parameter	Specification	Value		
Excitation laser	λ_e	488.0 nm	514.5 nm	532.0 nm
	Spot size at the waist (in the sample), $2\omega_{0e}$	61.3 μm	64.6 μm	60.1 μm
	Maximum laser power at cell	180 mW	175 mW	210 mW
Probe laser	λ_p	632.8 nm		
	Focusing lens focal length, f_p	185 mm		
	Rayleigh range, z_R	7.1 mm		
	Laser power at cell(s)	3 mW		
	Spot size at sample	108 μm		
Other parameters	Optical path length of cells	1 mm		
	Resolution of time-resolved curves	37.5 μs		
	Frequency	0.1–10 Hz (optimum 2 Hz)		
	Sample-to-detector distance	95 cm		

Beam Propagation Analyzer (Spiricon, Inc., Logan, UT) according to the steps of International Standards Organization no. 11 146 standard procedure.

The estimation of scattering effects of PMA platelets was performed with the thermal lens spectrometer with the modulated excitation beam at 514.5 nm in the absence of a probe beam. The intensity of the scattered light and the corresponding scattering was $A_s = I_e/I_{es}$, where I_e is the intensity of the incident excitation beam and I_{es} is the intensity of the detected scattered light at 90° to the beam-propagation axis. The latter value was detected by the photodiode (the stained-glass bandpass filter and the pinhole removed) in a continuous intensity detection mode similarly described.³⁰

Data Treatment. Thermal lens signal was acquired as a relative change in the probe-beam intensity¹⁴ $\vartheta(t) = [I_p(0) - I_p(t)]/I_p(t)$, according to the diffractive model as:

$$\begin{aligned} \vartheta(t) &= 4 \left(\frac{P_e}{\omega_{0e}^2} \right) \times B(t) \times E_0 D_T \times \alpha l \\ &= P_e \times \frac{B(t)}{t_c} \times E_0 \times 2.303 \varepsilon l c \end{aligned} \quad (1)$$

where $I_p(0)$ is the intensity of the probe beam at the photodetector plane in the central part of the beam at the time $t = 0$ (from this point on, the subscript “p” will denote the probe beam, and the subscript “e” will stand for the excitation beam), and $I_p(t)$ is the intensity of the probe beam at the moment t , P_e is the excitation-laser power, ω_{0e} is the excitation-beam waist radius, D_T is thermal diffusion coefficient, α is the linear absorption coefficient of the sample, ε is the molar absorptivity, and c is molar concentration of the absorbing substance in the sample. $B(t)$ is the time-dependent geometrical constant of the optical scheme³³

$$B(t) = \frac{1}{2} \tan^{-1} \left\{ \frac{2mV}{[(1+2m)^2 + V^2] \left(\frac{t}{2t} \right) + 1 + 2m + V^2} \right\} \quad (2)$$

Here, m is the ratio of cross-section areas of the probe and excitation beams at the sample, and V is the relative distance from the excitation waist to the sample. The factor E_0 is the enhancement factor of PT lensing for unit excitation-laser power:

$$E_0 = \frac{-dn}{dT} \frac{1}{\lambda_p k} \quad (3)$$

where k the thermal conductivity. t_c is the characteristic time of the thermal lens:

$$t_c = \frac{\omega_{0e}^2}{4D_T} \quad (4)$$

For steady-state measurements in a continuous-wave mode, Eq. 1 converts to

$$\theta = 2.303 B_\infty E_0 P_e \varepsilon l c \quad (5)$$

where θ is the steady-state PT signal corrected for the steady-state geometry constant $B_\infty = B(t \rightarrow \infty)$, $\theta = \vartheta/B_\infty$. Experimental values of sample absorbance A_{exp} were corrected to scattering $A = A_{\text{exp}} - A_s$. As well, experimental values of the PT signal θ were corrected to take into account a decrease in the excitation power due to light-scattering losses:

$$\theta_{\text{corr}} = \frac{\theta(A_{\text{exp}} + A_s)}{A_{\text{exp}}} \quad (6)$$

The recalculations of the absorbance from photothermal measurements (A_{PT}) were calculated from the equation deduced from Eq. 1 and the Beer’s law $A = \varepsilon l c$:

$$A_{\text{PT}} = \frac{\theta_{\text{corr}}}{2.303 E_0 P_e} \quad (7)$$

The experimental coefficient $2.303 E_0 P_e$ was measured by the previously developed approach for layered solids.³⁴ The minimum detectable linear absorption coefficients for photothermal and photometric (or SPS) measurements were calculated according to the equations previously deduced from the theory of these two methods for the conditions of shot noise determining the measurement precision.³⁰

$$\alpha_{\text{min}}^{\text{PT}} = \sqrt{\frac{2h\nu_p}{\eta P_p} \Delta f} \frac{B_\infty \omega_{0e}^2 \psi}{4P_e E_0 D_T l} \quad (8)$$

$$\alpha_{\text{min}}^{\text{SPS}} = \sqrt{\frac{h\nu_e}{\eta P_e} \Delta f} \frac{1}{l} \quad (9)$$

Here, h is Planck’s constant, ν_e and ν_p are frequencies of the excitation and probe beams, respectively; η is the detector quantum yield; Δf is the detection-channel bandwidth; other

parameters are listed above. The comparison of sensitivities for the same detector (η and Δf) and the same source of absorption–photothermal excitation is given by the equation simply deduced from Eqs. 8 and 9:

$$\alpha_{\min}^{\text{SPS}}/\alpha_{\min}^{\text{PT}} = \sqrt{\frac{v_e P_e P_p}{2v_p}} \frac{4E_0 D_T}{B_\infty \omega_{0e}^2 \psi} = E_0 D_T \times \frac{\sqrt{8\lambda_p/\lambda_e}}{B_\infty \omega_{0e}^2} \times \frac{\sqrt{P_p P_e}}{\psi} \quad (10)$$

The extraction percentage (R) and the distribution coefficient (D) of metals were calculated employing the equations

$$R = \frac{c_0 - c}{c_0} \times 100\% \quad (11)$$

and

$$D = \frac{R}{(100 - R)} \times \frac{V}{m_{\text{PMA}}} \quad (12)$$

where c_0 and c are the initial and final concentrations of analyte, respectively, in the solution (in moles per liter); V is the volume of the solution (in liters); m_{PMA} is the weight of the PMA platelet (in grams). The distribution coefficient of the metals toward PMA matrices was estimated for each metal at the corresponding optimal pH. Fifty milliliter solutions of 1 $\mu\text{g}/\text{mL}$ metal were shaken with 0.21/0.25 g PMA for 60 min to reach the equilibrium.

RESULTS AND DISCUSSION

Sorption ability of PMA matrices lies in target absorption in the mesopores formed as a result of occlusion of polyethylene glycols in the sorbent body during the polymerization process.^{23,24} Adsorption of the target substance from solution in these mesopores is facilitated by both electrostatic and steric effects. Thus, a photometric reaction is performed at the surfaces and within the mesoporous matrix, resulting in the analyte preconcentration and increasing path length compared with surface-enhanced matrices as the signal (photometric, fluorescent, or photothermal) is generated in the entire matrix.

Thermal Lens Tests of Polymethacrylate Matrices.

Laser-Induced Matrix Decomposition. Thermal lensing shows that colored PMA matrices exhibit a change in thermal lens signal during the measurement. It shows a short increase in the signal, followed by a longer and slower decrease (Fig. 2). Usually, such thermal lens experiments account for bleaching of the colored component of the matrix;^{14,23,24,35–37} however, Fe(II) *tris*(1,10-phenanthroline) is not photochemically active and thermally stable under such laser fluences.³⁵ Thus, this effect can result from the destruction of PMA itself due to local overheating. This first leads to local deformation (expansion) of the material, which results in an increase in the signal; this results in cavern formation, which was observed for the interaction of polymer materials with laser radiation.³⁸ Long exposure of PMA platelets result in completely irreproducible signals and caverns visible to the naked eye.

Thus, averaging thermal lens signal for times of several seconds usually practiced in solvent measurements in TLS is not suitable for these PMA matrices. Theoretical estimation, Eq. 5 and the signal corresponding to the decrease of the signal on Fig. 2, ϑ_0 , corresponds the expected thermal lens signal. For instance, for a sample with an absorbance of 0.225 for an

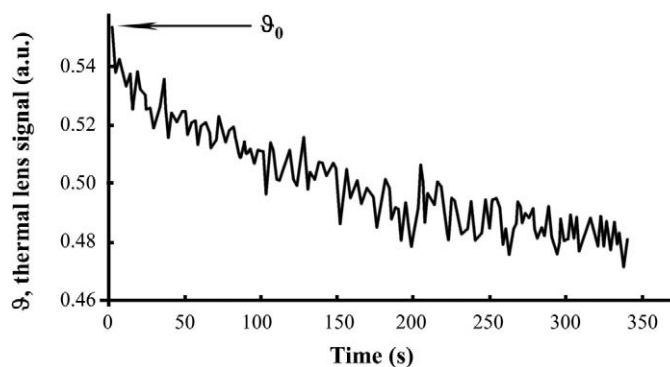


FIG. 2. Dependence of the thermal lens signal of a PMA platelet treated with procedure 4; Fe(II) concentration is 0.5 mg/L. Excitation power is 150 mW. ϑ_0 is the initial thermal lens signal of the sample.

excitation power of 150 mW, the initial thermal lens signal in PMA is 2.5 ± 0.3 , and the final plateau signal is 0.21 ± 0.01 ($n = 10$, $P = 0.95$), while the theoretical calculation for the spectrometer used (Table I) and experimental conditions (PMA plates with a thickness of 1.00 ± 0.01 mm) from Eq. 5 predicts a value of 2.8. Thus, the maximum sensitivity and precision are attained if the matrix is exposed to radiation for a short time, and only the first measurement results are taken into account.

Thus, a SPETLS procedure involving PMA matrices should include the optimization of the duration of the measurement of a single point. We have found that the measurement time that does not affect the matrix significantly (a change in the signal below 3%) at the selected laser fluence is 1–2 s (one to four thermal lens blooming–dissipating cycles, depending on the frequency). In all the following experiments, we used an exponential approximation of time-resolved thermal lens signals, Eq. 1, to estimate the initial values of the signal, which are in good agreement with the theory. Under these conditions, the quality of the analytical information should be enhanced by scanning the matrix surface, which also provides the information on the equality of the depth of the analytical reaction in PMA body.

Matrix Pretreatment. Although Eq. 1 predicts that thermal lens signal depends on the incident and absorbed energy and not affected by the light scattering,^{31,36} high light scattering decreases the excitation fluence and, hence, the signal.³⁹ Although mesoporous PMA matrices are highly transparent, the used platelets show considerable light scattering due to the defects in the course of polymerization and are accompanied by macrodefects, which result in the formation lens- or prism-like elements, thus degrading the thermal lens signal.

Thus, we used two approaches to improve the surface quality of PMA matrices prior thermal lens measurements, (1) a change in the conditions for matrix preparation, and (2) thermal improvement of the matrix surface. Thus, compared with previous SPS applications of PMA matrices,^{2,7,8,11–13,15–17,25–31} we used procedure 1, implementing the formation of PMA matrices between optical-quality glasses. For thermal treatment, we developed procedure 2, which is based on heating the surface of a PMA matrix after treating with the reagent and performing the analytical reaction through a flat optical glass; it provides local redistribution of the polymer drastically diminishing the surface defects. Figure 3 shows absorption spectra of matrices filled with 1,10-phenanthroline (procedure 3)

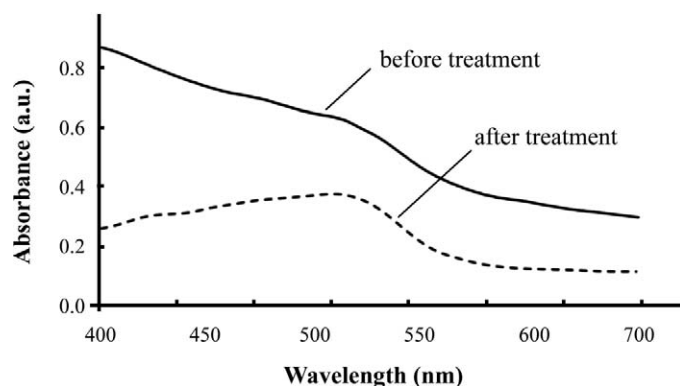


Fig. 3. Absorption spectra (against air) of a PMA platelet filled with Fe(II) *tris*(1,10-phenanthroline) (procedure 4). The thermal treatment of platelets was made according to procedure 2.

and in contact with an Fe(II) solution before and after such a thermal treatment. All subsequent results were obtained for PMA matrices by implementing these treatment procedures. After this treatment, scattering effects were considerably decreased and were no more than 1–2% of the transmitted light. Under these conditions, the distortions in thermal lens signal were negligible, and the values of absorbances calculated from thermal lensing, Eq. 7 were in good agreement with the absorbances from SPS measurements.

Mercury(II) and Iron(II). The absorption spectrum of immobilized copper dithizonate shows an absorption maximum at 540 nm. On the interaction with trace mercury, the adsorption spectrum in a polymer phase has a maximum at 490 nm and corresponds to the absorption spectrum of Hg(II) dithizonate. The sampling procedure (procedure 3) is rapid and takes about 15 min, requiring no complicated equipment. The determination of mercury is not interfered with 100-fold excess amounts of Fe(II, III), Pb(II), Ni(II), Zn(II), Co(III), Cd(II), and Cu(II), which usually accompany mercury in many samples. Thus, the proposed method is very selective.

Such a nonlinear dependence of solution absorbance on the mercury concentration is determined by the character of solid-phase reaction of mercury with PMA. Previously, we found that this process is well described with the Freundlich equation—the limit of detection of mercury by absorption spectroscopy is 1×10^{-7} M (20 ng/mL).³⁷ Under the same conditions, the thermal lens signal (488.0 nm, 100 mW of the excitation laser) shows a linear calibration range from 2.0×10^{-9} to 1.0×10^{-5} M Hg(II) ($r = 0.9881$, $n = 8$), with a slope of 19.6 (Fig. 4, curve 1). The slope enhancement is 40, which is in good agreement with the theoretical estimation for the conditions of procedure 3. The SPETLS limit of detection of mercury is 1×10^{-8} M (the estimated value of the minimum detectable absorbance is 1×10^{-4}), which provides a 10-fold enhancement compared with SPS. It is noteworthy that the upper determination limit of mercury is the same as in conventional absorbance measurements.

The procedure for the determination of Fe(II) with 1,10-phenanthroline is the same in principle, although is somewhat less sensitive due to the lower molar absorptivity of this chelate (Fig. 4, curve 2). The absorption spectra show a characteristic peak shape of Fe(II) *tris*(1,10-phenanthroline). No changes in the analytical procedure (procedure 3) are needed. The sensitivity coefficient enhancement compared with SPS is

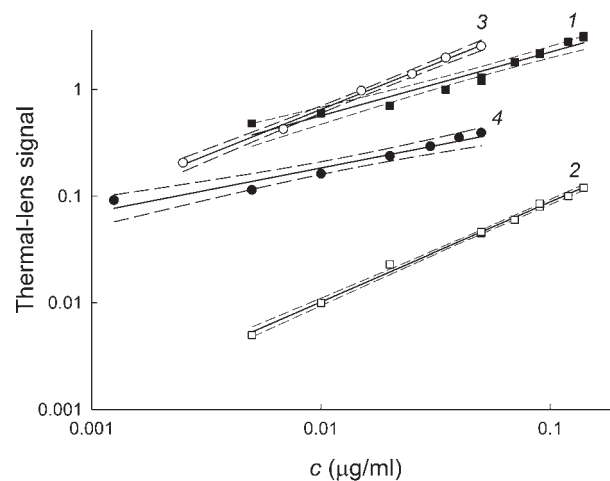


Fig. 4. Solid phase-enhanced thermal lens calibration plots (dashed lines show confidence intervals) for Hg(II) (immobilized reagent is Cu dithizonate; 488.0 nm, 100 mW), black squares, 1; Fe(II) (1,10-phenanthroline; 514.5 nm, 120 mW) white squares, 2; Cu(II) (Pb(II) diethyldithiocarbamate; 514.5 nm, 40 mW) white rounds, 3; and Ag^I (dithizone; 514.5 nm, 40 mW), black rounds, 4; in PMA-based matrices (1-mm path length).

47.0, which is also in good accordance with the estimation from Eq. 10), and the limit of detection of iron is 1×10^{-7} M (the estimated value of the minimum detectable absorbance is 4×10^{-4}), with a linear calibration (Fig. 4) range from 9.0×10^{-8} to 3.0×10^{-5} M Fe(II) ($r = 0.9903$, $n = 11$).

Silver(I) and Copper(II). For SPETLS measurements of Ag(I) and Cu(II), it is necessary to decrease the concentration of the test element in PMA, as the linear dependence of the thermal lens signal on absorbance deviates^{14,40} and high absorbances degrade the sensitivity. The simplest way was to change the analytical conditions is decreasing the time of contact of the PMA platelet modified with dithizone and Pb(II) diethyldithiocarbamate (procedure 3). Apart from this, other significant changes in the procedures are not needed, and the linearity of calibration is good as in the previous cases (Fig. 4, curve 3). The thermal lens limits of detection are decreased by an order compared with SPS to 10^{-8} M.⁴¹ It is important that the same decrease in SPETLS limits of detection for silver and copper is attained for lower excitation power compared with Fe(II) and Hg(I), although changes in the calibration slopes are different (Fig. 4, curve 4). In our opinion, this means that at high excitation powers, the laser still affects the matrix, increasing the error of the measurements, and this error compensates for the increase in the calibration slope. This was confirmed by the estimation of the limit of detection of Fe(II) with 1,10-phenanthroline at the excitation power of 40 mW. The value is 8×10^{-8} M, which is only 25% higher than for procedure 3, while the excitation power is threefold lower.

The developed procedures provide rather high sensitivity compared with common (solution based) spectrophotometry due to the advantageous parameters of preconcentration of elements in matrices. Table II shows the distribution coefficients of metals in PMA matrices, which are rather high. High distribution coefficients were attained not only for metals, but also for organic substances like bromocresol green ($D = 110$), which shows the versatility of the approach. Taking into account the volume ratio of the initial solution and the mesoporous matrix, the degree of preconcentration is high,

TABLE II. Distribution coefficients (D) for the procedures developed (sample volume 50 mL, $m_{\text{PMA}} = 0.21 \div 0.25$ g, $c_{\text{M}} = 1$ $\mu\text{g/mL}$).

Metal	D (mL \times g $^{-1}$)
Cu	1303
Ag	741
Fe	438

which provides advantageous analytical parameters of the procedures (see Table III⁴²⁻⁵²).

Indirect Determination of Ascorbic Acid. We studied the interaction of the immobilized 2,6-dichlorophenolindophenol with ascorbic acid for assessing the possibility of using the material obtained for indirect photothermal determination of ascorbic acid. The color intensity of the PMA matrix with immobilized 2,6-dichlorophenolindophenol decreases after its contact with the ascorbic acid solution.²⁷ The study of the effect of the pH of the ascorbic acid solution showed that the decrease in absorbance was the largest at pH 3, which is similar to absorbance measurements.²⁵ Thus, changes in photometric procedures are needed. The dependence of the decrease in the thermal lens signal at 514.5 nm, $\Delta\vartheta_{514.5}$, on the concentration of ascorbic acid at pH 3, and the contact time of 15 min are presented in Fig. 5. The calibration curve is described by the equation $\Delta\vartheta_{514.5} = (0.009 \pm 0.002) + (5.48 \pm 0.07)c_{\text{asc}}$ ($P = 0.95$, $n = 7$, $r = 0.996$), where c_{asc} is the concentration of ascorbic acid (in milligrams per liter). The limit of detection is 7×10^{-7} M. Thus, the use of SPETLS for indirect determination with a PMA-immobilized reagent provides a decrease in the limit of detection by an order compared with SPS determination under the same conditions.³⁷ In addition, this example shows that SPETLS can be used for the determination of analytes, based on redox reactions. Both factors can be used for the implementation of previously unused indirect redox photometric determinations in SPETLS.

Photothermal Versus Photometric Sensitivity Comparison for Polymethacrylate Matrices. The problem of estimating the performance parameters of analytical procedures prior measurements is a very topical problem in TLS, as it provides the correct selection of photometric reaction as the legacy of spectrophotometry. The simplest way is to use the Eq. 7, as the term $2.303E_0P_e$ is an increase in the sensitivity when shifting from absorbance measurements to PT techniques. However, this is too straightforward an approach: First, as it takes into account the calibration slope only, which is a less crucial analytical parameter compared with the limit of detection. Second, it shows estimation for steady-state thermal lens experiments only and does not take into account the chopper frequency or excitation-beam focusing, which can be very important for the sensitivity of thermal lensing.¹⁹

Contrary to this approach, Eq. 10 provides a more correct way of comparison, as it is based on the minimum absorption coefficients, i.e., the limits of detection, and takes into account a much larger group of parameters. This comparison shows that the ratio of instrumental limits of detection for photometric and PT measurements does not depend on the detector parameters (η and Δf) and relies on thermo-optical properties of the sample E_0 and D_T (first term) and the setup parameters (beam wavelengths, beam focusing, and setup geometry, second term), and chopper frequency and beam power (third term). We

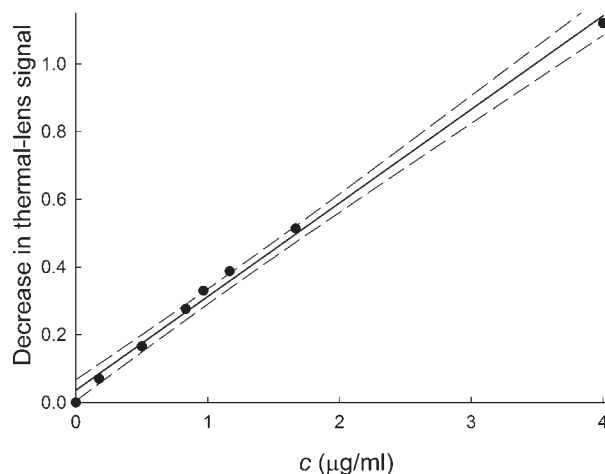


FIG. 5. Indirect solid-phase-enhanced thermal lens calibration plots (dashed lines show confidence intervals) for ascorbic acid by a decrease in the thermal lens signal of the immobilized reagent (2,6-dichlorophenolindophenol, 514.5 nm, 40 mW) in PMA-based matrices (1 mm pathlength).

separate the second and third terms as the frequency and beam powers are changeable parameters in the experiment.

Another question arising from this equation is the optimization of the number of thermal lens excitation cycles per point of the platelet: As Eq. 10 shows, an increase in the sensitivity is inversely proportional to the excitation frequency; however, lower frequencies mean lower number of cycles and, hence, lower data volume. On the other hand, as we have shown above, the thermal degradation of the matrix does not allow for a long excitation times. Thus, an optimum should be found. The experiments with Fe(II) (see procedure 3 and its discussion below) showed the optimum of 2 Hz excitation, which provided four to five replicate measurements of the thermal lens signal, making reliable measurements for any point of the platelet.

According to Eq. 10, it is possible to compare the sensitivity of photometric and photothermal measurements and for the same detector and the same laser used for measuring absorption and photothermal excitation. This shows that for the experimental conditions (Table I), the minimum detectable linear absorption coefficient in SPETLS is about 50-fold lower than for conventional photometry. This means that the maximum increase in the SPETLS sensitivity will be attained for analytical reactions with colorless reagents (such as 1,10-phenanthroline), while a color-reagent system might demand diminishing the reagent amount and thus modify the analytical procedure.

Comparison of Analytical Possibilities of the Technique.

The comparison of all the SPETLS procedures with mesoporous PMA matrices, we can state that optimized measurement conditions in these matrices provide a 50-fold increase in the calibration slopes and a ten-fold decrease in the limits of detection compared with spectrophotometry, under the same conditions due to the thermo-optical properties of PMA. The calibration range covers 3–4 orders of magnitude. Figures 4 and 5 show that in all the cases the linearity is good, and narrow confidence intervals (dashed lines) are achieved. The comparison of the proposed procedures with the existing methods for optical and sensor-based applications for the selected analytes (Table III) shows that SPETLS limits of

TABLE III. Comparison of performance parameters of the proposed methods based on mesoporous polymethacrylate matrices with other methods. Excitation power in photothermal experiments is 40 mW for metals and 30 mW for ascorbic acid.

Analyte	Method	Linear range (mol/L)	Detection limit ($\mu\text{mol/L}$)	Reference
Cu	Optical sensor (triacetylcellulose membrane)	8.3×10^{-7} to 1.6×10^{-5}	0.2	48
	Optical sensor (PVC membrane)	6.3×10^{-7} to 1.0×10^{-4}	0.33	49
		1×10^{-6} to 1×10^{-2}	N/A ^a	50
	Optical sensor (Amberlite XAD-2 polymer)	7.8×10^{-5} to 2.0×10^{-3}	N/A	51
	Reflectance spectroscopy (silica gel)	4.7×10^{-7} to 2.5×10^{-5}	0.047	46
	Solid phase spectrophotometry (PMA matrices)	7.8×10^{-7} to 1.6×10^{-5}	0.23	This work
Ag	Photothermal lensing (PMA matrices)	1×10^{-7} to 1.4×10^{-6}	0.03	
	Optical sensor (triacetylcellulose membrane)	1.8×10^{-6} to 5.6×10^{-5}	0.8	52
	Optical sensor (PVC membrane)	1×10^{-6} to 1×10^{-1}	N/A	50
	Reflectance spectroscopy (silica gel)	4.6×10^{-7} to 1.0×10^{-5}	0.028	46
	Solid phase spectrophotometry (PMA matrices)	4.6×10^{-7} to 7.4×10^{-6}	0.37	This work
		1.8×10^{-7} to 1.8×10^{-6}	0.09	
Hg	Photothermal lensing (PMA matrices)	2×10^{-8} to 1×10^{-6}	0.01	
	Optical sensor (triacetylcellulose membrane)	2.4×10^{-5} to 4.7×10^{-4}	7.2	42
		7.5×10^{-7} to 9.7×10^{-6}	0.1	43
	Flow-through optrode (PVC membrane)	1.0×10^{-5} to 1.0×10^{-3}	0.54	44
	Solid phase spectrophotometry (PMA matrices)	1.0×10^{-7} to 1.0×10^{-6}	0.1	This work
	Photothermal lensing (PMA matrices)	3×10^{-8} to 1×10^{-5}	0.01	
Fe	Solid phase spectrophotometry (polyurethane)	1.0×10^{-4} to 1.0×10^{-3}	3.7	45
	Reflectance spectroscopy (silica gel)	4.8×10^{-6} to 2.7×10^{-4}	1.4	46
	Solid phase spectrophotometry (PMA matrices)	3.0×10^{-6} to 8.9×10^{-5}	3	This work
		8.9×10^{-7} to 3.6×10^{-5}	3	
Ascorbic acid	Photothermal lensing (PMA matrices)	1.0×10^{-7} to 1×10^{-5}	0.1	
	Optical sensor (Amberlite XAD-2 polymer)	1.6×10^{-3} to 1.0×10^{-2}	N/A	47
	Solid phase spectrophotometry (PMA matrices)	2.8×10^{-5} to 2.8×10^{-4}	3	This work
	Photothermal lensing (PMA matrices)	4×10^{-6} to 5×10^{-5}	0.7	

^aN/A = not applicable.

detection are lower than the majority of the optical methods based on diffuse-reflectance spectroscopy and several membrane sensors. This is a result of both the advantages of the developed procedures in PMA matrices and the photothermal signal enhancement in PMA. It is worth mentioning that SPETLS shows rather good linearity (especially for Hg, Fe, and Ag), excelling that of other sensors and their SPS counterparts.

It is important that the SPETLS limits of detection depend on the excitation power only slightly, and good performance parameters are attained for excitation powers of 30 to 40 mW (Table III), which are characteristic for state-of-the-art diode lasers, i.e., SPETLS can be used as compact laser-diode-based photothermal lens devices for rapid tests and analysis.

However, Figs. 4 and 5 correspond to photometric reactions unchanged compared with previous SPS studies,^{23,25–29} and these procedures are rather flexible. As PMA matrices allow for the preconcentration, changing the time of contact of reagent-modified PMA platelet with the solution to be analyzed, and the contact mode (batch conditions, stirring, etc.) can change the performance parameters. For instance, Fig. 6 shows three calibrations for Fe(II) for the time of contact of the test Fe(II) solution with the PMA platelets for 15 min (procedure 3, as above) and with changed contact times. It shows that extending the contact time increase the amount of iron preconcentrated on the platelet, increasing the slope (Fig. 6, curve 2) and decreasing the limit of detection to 3×10^{-8} M, while decreasing the time of contact to 5 min degrades the limit of detection but provides the determination of Fe(II) with appropriate accuracy for an extra order of the magnitude. This feature is much more promising in SPETLS compared with SPS, as the error curve for both methods is significantly

different, and thermal lensing provides a wider calibration range.¹⁴

Finally, the properties of PMA matrices with immobilized reagents are stable for not less than a month^{23,25–29} and can be used as so-called complete analytical forms. These optical elements could be used in a wide range of applications for preconcentration of trace elements by solid-phase extraction methods and determination of elements in a solid phase by a combination photometric, photothermal, or visual indication of the analytical signal, or a combination.

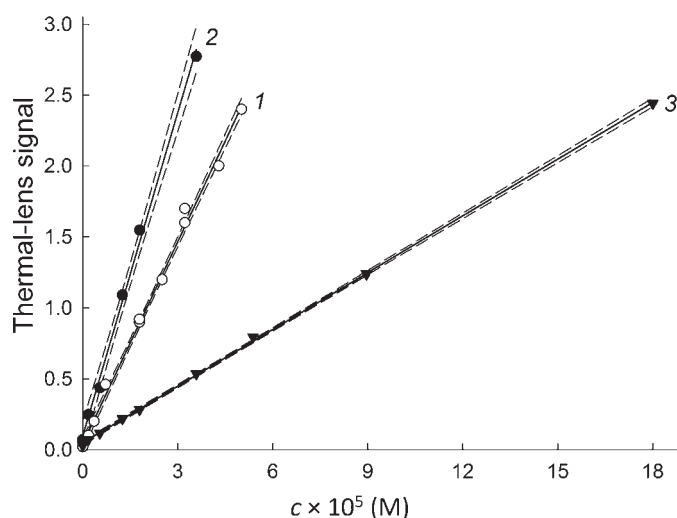


Fig. 6. Thermal lens calibration plots (dashed lines show confidence intervals) for Fe(II) (immobilized reagent is 1,10-phenanthroline; 514.5 nm, 120 mW) in PMA-based matrices (1 mm pathlength) depending on the time of contact of the test solution with PMA platelet: 1, 15 min (procedure 4); 2, 30 min; and 3, 5 min.

CONCLUSION

As a whole, we showed that solid phase-enhanced photo-thermal lens spectroscopy can be successfully used with photometric reactions in the bulk of mesoporous PMA, with a significant increase in the sensitivity. The advantages of this approach are (i) in designing and developing a solid-phase reaction, one can select from virtually the whole multitude of known color-developing (photometric) reactions previously worked out for most elements, and all the major classes of organic substances and biomarkers; (ii) solid-phase mesoporous PMA matrices are more stable than solutions, thus unstable samples can be measured or their storage is easy; (iii) sampling is rapid (takes about 15 min, procedures 3 and 4), without any complicated equipment as the main part of photometric analysis is included in the design of the sensing material; (iv) as the mesoporous nature of the matrix allows quick conditioning, these materials can be easily used in batch conditions and in the flow with a minimum change in sampling-sample preparation, and therefore, the development of photometric methods is made quicker and easier; and (v) these matrices can be used for the preconcentration of substances from solutions as well as from gas phases (gases and aerosols). Note that the preconcentration stage is also an intrinsic part of color development; we have higher sensitivity compared with conventional photometry. By adding the sensitivity of photothermal measurements, it is possible to introduce this spectrochemical technique in flow analysis, fiber-optical sensors gas/solute optical or photothermal devices, and in microfluidics and state-of-the-art separation methods.

ACKNOWLEDGMENTS

The work was supported by the Russian Foundation for Basic Research, grants nos. 10-03-01018-a; 08-03-90714-mob_st; 09-03-90756-mob_st; 09-03-90758-mob_st; 10-03-90752-mob_st, 11-03-90737-mob_st, and 12-03-90842-mol_rf_nr and the Ministry of Science and Technology of Russian Federation, contract nos. 16.740.11.0471, P990, 16.740.11.0334, and 02.444.11.7141.

1. R. Narayanaswamy, O.S. Wolfbeis. *Optical Sensors. Industrial, Environmental and Diagnostic Applications*. Berlin Heidelberg, Germany: Springer, 2004.
2. N.A. Gavrilenko, G.M. Mokrousov, O.V. Dzhiganskaya. "An Optical Sensor for the Determination of Ascorbic Acid". *J. Anal. Chem. (Russ)*. 2004. 59(9): 871-874.
3. G.D. Brykina, V.V. Rybalka, S.G. Dmitrienko, O.A. Shpigun. "Sorption of Bilirubin and its Determination by Solid-State Spectrophotometry". *J. Anal. Chem. (Russ)*. 1994. 49(2): 162-167.
4. S. Saputro, K. Yoshimura, S. Matsuoka, K. Takehara, Narsito. "Improved Solid-Phase Spectrophotometry for the Microdetermination of Chromium(VI) in Natural Water". *Anal. Sci.* 2009. 25(12): 1445-1450. doi:10.2116/analsci.25.1445.
5. A.S. Amin. "Utilization of Solid-Phase Spectrophotometry for the Determination of Trace Amounts of Copper Using 5-(2-Benzothiazolylazo)-8-hydroxyquinoline". *Chem. Papers*. 2009. 63(6): 625-634. doi:10.2478/s11696-009-0067-x.
6. A.S. Amin, A.A. Gouda. "Utility of Solid-Phase Spectrophotometry for Determination of Dissolved Iron(II) and Iron(III) Using 2,3-Dichloro-6-(3-carboxy-2-hydroxy-1-naphthylazo)quinoxaline". *Talanta*. 2008. 76(5): 1241-1245. doi:10.1016/j.talanta.2008.05.034.
7. G.M. Mokrousov, N.A. Gavrilenko, T.I. Izaak, N.G. Garber. "Sensitive Polymethylacrylate-Based Element for a Moisture Sensor". *Russ. J. Appl. Chem.* 2000. 73(9): 1643-1645.
8. M.A. Gavrilenko, N.A. Gavrilenko, G.M. Mokrousov. "Solid-Phase Extraction of Aliphatic Amines from the Aqueous Phase with a Methacrylate Polymer". *Russ. J. Appl. Chem.* 2005. 78(9): 1408-1410. doi:10.1007/s11167-005-0527-1.
9. S. Taguchi, H.F. Sun, N. Hata, I. Kasahara. "Design of Simple and Sensitive Methods for Trace Analysis by Means of Concentration with a Membrane Filter". *Bunseki Kagaku*. 2000. 49(12): 941-952.
10. C.M. Hill, K.W. Street, S.P. Tanner, W.H. Philipp. "Preparation of Ion Exchange Films for Solid-Phase Spectrophotometry and Solid-Phase Fluorometry". *Anal. Lett.* 2000. 33(13): 2779-2792.
11. N.A. Gavrilenko, G.M. Mokrousov. Sensitive Indicator Material for Determining Substance Microquantities. Russian Patent WO/2006/025763. Filed March 09, 2006.
12. M.A. Gavrilenko, N.A. Gavrilenko. "Polymethacrylate Sorbent for the Solid-Phase Extraction of Amines". *Mendelev Comm.* 2006. 16(2): 117-119. doi:10.1070/MC2006v016n02ABEH002125.
13. E.V. Anishchenko, N.S. Eremina, N.A. Gavrilenko, G.M. Mokrousov. "Influence of the Silver Ions on the Physicochemical Properties of Methyl Methacrylate-Methacrylic Acid Copolymer Films". *Russ. J. Appl. Chem.* 2006. 79(3): 453-456. doi:10.1134/s1070427206030244.
14. S.E. Bialkowski. *Photothermal Spectroscopy Methods for Chemical Analysis*. New York: Wiley-Interscience, 1996.
15. G.M. Mokrousov, N.A. Gavrilenko, N.G. Garber, M.A. Gavrilenko. "Intermolecular Interactions in Poly(methyl methacrylate) Modified with Silver, Copper, or Neodymium Trifluoroacetates". *Russ. J. Phys. Chem.* 2001. 75(6): 1023-1025.
16. G.M. Mokrousov, N.A. Gavrilenko, N.S. Eremina, N.G. Garber. "Effect of Metal Trifluoroacetates on the Thermal Decomposition of Poly(methyl methacrylate)". *Russ. J. Phys. Chem.* 2001. 75(6): 1026-1028.
17. D.A. Nedosekin, W. Faubel, M.A. Proskurnin, U. Pyell. "Determination of Light-Absorbing Layers at Inner Capillary Surfaces by CW Excitation Crossed-Beam Thermal Lens Spectrometry". *Talanta*. 2009. 78(3): 682-690. doi:10.1016/j.talanta.2008.12.020.
18. D.A. Nedosekin, A.V. Pirogov, W. Faubel, U. Pyell, M.A. Proskurnin. "Investigation of Ionene Adsorption on Quartz Surfaces by Thermal Lens Spectrometry". *Talanta*. 2006. 68(5): 1474-1481. doi:10.1016/j.talanta.2005.08.010.
19. A. Smirnova, M.A. Proskurnin, S.N. Bendrysheva, D.A. Nedosekin, A. Hibara, T. Kitamori. "Thermo-optical Detection in Microchips: From Macro- to Micro-scale with Enhanced Analytical Parameters". *Electrophoresis*. 2008. 29(13): 2741-2753. doi:10.1002/elps.200700914.
20. M.A. Proskurnin, V.V. Chernysh, V.A. Filichkina. "Some Metrological Aspects of the Optimization of Thermal Lens Procedures". *J. Anal. Chem. (Russ)*. 2004. 59(9): 818-827. doi:10.1023/B:JANC.0000040695.95051.be.
21. N.A. Gavrilenko, N.V. Saranchina. "Analytical Properties of 1-(2-Pyridylazo)-2-Naphthol Immobilized on a Polymethacrylate Matrix". *J. Anal. Chem. (Russ)*. 2009. 64(3): 226-230. doi:10.1134/s1061934809030034.
22. N.A. Gavrilenko, N.V. Saranchina. "Solid-Phase Spectrophotometric Determination of Silver Using Dithizone Immobilized in a Polymethacrylate Matrix". *J. Anal. Chem. (Russ)*. 2010. 65(2): 148-152. doi:10.1134/s1061934810020085.
23. M.A. Gavrilenko, N.A. Gavrilenko, G.M. Mokrousov. "Preconcentration of Phenols on a Polymethacrylate Sorbent for Their Gas-Chromatographic Determination in Water". *J. Anal. Chem.* 2006. 61(3): 216-218. doi:10.1134/S1061934806030038.
24. M.A. Gavrilenko, G.M. Mokrousov, O.V. Dzhiganskaya. "An Optical Sensor for Determination of Ascorbic Acid". *J. Anal. Chem. (Russ)*. 2004. 59(9): 871-874. doi:10.1023/B:JANC.0000040703.73042.61.
25. N.A. Gavrilenko, N.V. Saranchina, G.M. Mokrousov. "A Sensitive Optical Element for Mercury(II)". *J. Anal. Chem. (Russ)*. 2007. 62(9): 832-836. doi:10.1134/s1061934807090043.
26. N.A. Gavrilenko, O.V. Mokhova. "Sorption-Spectrophotometric Determination of Iron(II, III) with the Use of Organic Reagents Immobilized in a Polymethacrylate Matrix". *J. Anal. Chem. (Russ)*. 2008. 63(11): 1038-1043. doi:10.1134/s106193480811004x.
27. N.A. Gavrilenko, A.V. Sukhanov, O.V. Mokhova. "Redox and Acid-Base Properties of 2,6-Dichlorophenolindophenol Immobilized on a Polymethacrylate Matrix". *J. Anal. Chem. (Russ)*. 2010. 65(1): 17-20. doi:10.1134/s1061934810010041.
28. G.M. Mokrousov, N.A. Gavrilenko, T.I. Izaak. "Ionic Conductivity of Polymethyl Methacrylate-Metal Trifluoroacetate Composites". *Russ. J. Appl. Chem.* 2000. 73(8): 1424-1426.
29. M. Galkin, V. Ageeva, D. Nedosekin, M. Proskurnin, A. Olenin, G. Mokrousov. "Thermal Lens Spectrometry for the Synthesis and Study of Nanocomposites on the Basis of Silver Salts Absorbed by a Polyacrylate Matrix". *Moscow University Chemistry Bulletin*. 2010. 65(2): 91-97. doi:10.3103/s0027131410020070.
30. D.A. Nedosekin, A.V. Brusnichkin, A.Y. Luk'yanov, S.A. Eremin, M.A. Proskurnin. "Heterogeneous Thermal Lens Immunoassay for Small Organic Compounds: Determination of 4-Aminophenol". *Appl. Spectrosc.* 2010. 64(8): 942-948. doi:10.1366/000370210792081136.
31. M.A. Proskurnin, V.V. Kuznetsova. "Optimisation of the Optical Scheme

- of a Dual-Beam Thermal Lens Spectrometer Using Expert Estimation". *Anal. Chim. Acta.* 2000. 418(1): 101-111. doi:10.1016/S0003-2670(00)00949-1.
32. I.V. Pyatnitskii, V.V. Sukhan. *Analytical Chemistry of Silver.* (Engl. Trans.). Moscow, the USSR: Nauka, 1975.
 33. R.D. Snook, R.D. Lowe. "Thermal Lens Spectrometry—A Review". *Analyst.* 1995. 120(8): 2051-2068. doi:10.1039/an9952002051.
 34. D.A. Nedosekin, M.A. Proskurnin, M.Y. Kononets. "Model for Continuous-Wave Laser-Induced Thermal Lens Spectrometry of Optically Transparent Surface-Absorbing Solids". *Appl. Optics.* 2005. 44(29): 6296-6306. doi:10.1364/ao.44.006296.
 35. A. Gaiduk, M. Yorulmaz, P.V. Ruijgrok, M. Orrit. "Room-Temperature Detection of a Single Molecule's Absorption by Photothermal Contrast". *Science.* 2010. 330(6002): 353-356. doi:10.1126/science.1195475.
 36. A.Y. Luk'yanov, G.B. Vladykin, M.A. Novikov, Y.I. Yashin. "Comparison of the Capability Limits of Some Optical Detectors for Liquid Chromatography". *J. Anal. Chem. (Russ).* 1999. 54(7): 633-638.
 37. A. Chartier, S.E. Bialkowski. "Accurate Measurements of Organic Dye Solutions by Use of Pulsed Laser Photothermal Deflection Spectroscopy". *Anal. Chem.* 1995. 67(15): 2672-2684. doi:10.1021/ac00111a028.
 38. M. Pons, S. Nonell, I. Garcia-Moreno, A. Costela, R. Sastre. "Time-Resolved Thermal Lens Study on the Heat Dissipation Effects in Solid Polymeric Matrices Used as Laser Dyes". *Appl. Phys. B Lasers Optics.* 2002. 75(6-7): 687-694. doi:10.1007/s00340-002-1028-z.
 39. H. Einsiedel, S. Mittler-Neher. "Polarization-Dependent Photothermal Beam Deflection for the Determination of the Order Parameter C_2 in a Laser-Oriented Polymer System". *Appl. Optics.* 1996. 35(27): 5406-5411. doi:10.1364/AO.35.005406.
 40. A.A. Schilt. *Analytical Application of 1,10-Phenanthroline and Related Compounds.* Oxford, UK: Pergamon, 1969.
 41. G.W. Ewing. *Instrumental Methods of Chemical Analysis.* New York: McGraw-Hill, 1985. 5 ed.
 42. H. Tavallali, E. Shaabanpur, P. Vahdati. "A Highly Selective Optode for Determination of Hg (II) by a Modified Immobilization of Indigo Carmine on a Triacetylcellulose Membrane". *Spectrochim. Acta Molecular Biomolecular Spectrosc.* 2012. 89: 216-221. doi:10.1016/j.saa.2011.12.055.
 43. A. Safavi, M. Bagheri. "Design and Characteristics of a Mercury(II) Optode Based on Immobilization of Dithizone on a Triacetylcellulose Membrane". *Sensor Actuator B Chem.* 2004. 99(2, 3): 608-612. doi:10.1016/j.snb.2004.01.022.
 44. C. Sanchez-Pedreno, J.A. Ortuno, M.I. Albero, M.S. Garcia, M.V. Valero. "Development of a New Bulk Optode Membrane for the Determination of Mercury(II)". *Anal. Chim. Acta.* 2000. 414(1-2): 195-203. doi:10.1016/S0003-2670(00)00809-6.
 45. R.J. Cassella. "On-line Solid-Phase Extraction with Polyurethane Foam: Trace-Level Spectrophotometric Determination of Iron in Natural Waters and Biological Materials". *J. Environ. Monitor.* 2002. 4(4): 522-527. doi:10.1039/b204700d.
 46. O. Zaporozhets, O. Gawer, V. Sukhan. "Determination of Fe(II), Cu(II) and Ag(I) by Using Silica Gel Loaded with 1,10-Phenanthroline". *Talanta.* 1998. 46(6): 1387-1394. doi:10.1016/S0039-9140(98)00007-1.
 47. G. Goodlet, R. Narayanaswamy. "An Optical-Fiber Vitamin C Sensor—Based on Immobilized 2,6-Dichloroindophenol". *Meas. Sci. Technol.* 1994. 5(6): 667-670. doi:10.1088/0957-0233/5/6/006.
 48. A. Safavi, M. Bagheri. "Design of a Copper(II) Optode Based on Immobilization of Dithizone on a Triacetylcellulose Membrane". *Sensor Actuator B Chem.* 2005. 107(1): 53-58. doi:10.1016/j.snb.2004.10.062.
 49. B. Rezaei, H. Hadadzadeh, A. Azimi. "Fabrication of an Optical Sensor Based on the Immobilization of Qsal on the Plasticized PVC Membrane for the Determination of Copper(II)". *J. Anal. Chem. (Russ).* 2012. 67(8): 687-693. doi:10.1134/s1061934812080060.
 50. X. Liu, Y. Qin. "Ion-Exchange Reaction of silver(I) and Copper(II) in Optical Sensors Based on Thiaglutaric Diamide". *Anal. Sci.* 2008. 24(9): 1151-1156. doi:10.2116/analsci.24.1151.
 51. N. Mahendra, P. Gangaiya, S. Sotheeswaran, R. Narayanaswamy. "Investigation of a Fiber Optic Copper Sensor—Based on Immobilised α -Benzoioxime (Cupron)". *Sensor Actuator B Chem.* 2003. 90(1-3): 118-123. doi:10.1016/S0925-4005(03)00044-3.
 52. S. Rastegarzadeh, V. Rezaei. "A Silver Optical Sensor Based On 5(*p*-Dimethylaminobenzylidene)rhodanine Immobilized on a Triacetylcellulose Membrane". *J. Anal. Chem. (Russ).* 2008. 63(9): 897-901. doi:10.1134/S1061934808090189.

Queries for apls-67-07-05

This manuscript/text has been typeset from the submitted material. Please check this proof carefully to make sure there have been no font conversion errors or inadvertent formatting errors. Allen Press.